

Development of a new thermoelectric $\text{Bi}_2\text{Ca}_2\text{Co}_{1.7}\text{O}_x$ + $\text{Ca}_3\text{Co}_4\text{O}_9$ composite

Sh. Rasekh^{1*}, N.M. Ferreira², F.M. Costa², G. Constantinescu¹, M.A. Madre¹, M. A. Torres³, J.C. Diez¹, A. Sotelo¹

¹ICMA (CSIC-Universidad de Zaragoza), Dpto. de Ciencia de Materiales, C/María de Luna 3, 50018-Zaragoza (Spain).

²i3N, Departamento de Física, Universidade de Aveiro, 3810-193 Aveiro, Portugal.

³Universidad de Zaragoza, Dpto. de Ingeniería de Diseño y Fabricación, C/María de Luna 3, 50018-Zaragoza (Spain).

Abstract

$\text{Bi}_2\text{Ca}_2\text{Co}_{1.7}\text{O}_x$ nominal composition ceramic rods were textured by the Electrically Assisted Laser Floating Zone technique. A new composite formed by three phases, two of them with well known thermoelectric properties, $\text{Bi}_2\text{Ca}_2\text{Co}_{1.7}\text{O}_x$ and $\text{Ca}_3\text{Co}_4\text{O}_9$, has been obtained for the first time when the growth process is performed with 300 mA applied current. Under these conditions the thermoelectric performances of this new composite reach values above the highest ones reported in the literature for polycrystalline $\text{Bi}_2\text{Ca}_2\text{Co}_{1.7}\text{O}_x$ materials.

Keywords: Directional solidification, Electrical resistivity, Electroceramics, Thermoelectric materials, Cobaltites

Corresponding author: Sh. Rasekh. E-mail: sh.rasekh@unizar.es. Tel.: +34 976762617; Fax: +34 976761957

Thermoelectric (TE) power generation is a promising technology to harvest wasted heat from different energy transformation systems. As a consequence, it can be very useful in order to reduce CO₂ emissions, helping to reach a global warming solution. For these applications, TE materials with high efficiency are required to be used in commercial devices. The performances of these materials are usually quantified by the dimensionless figure of merit, ZT, defined as $TS^2/\rho\kappa$ (where S is the Seebeck coefficient, T the absolute temperature, ρ the electrical resistivity and κ the thermal conductivity; S^2/ρ is the power factor, PF). From this definition, a high performance TE material should possess high Seebeck coefficient, with low electrical resistivity and thermal conductivity [1].

For the past decades, high ZT intermetallic materials have been widely applied in various sectors, e.g. automobile industry. Nonetheless, these materials have some drawbacks, as their low stability at high temperature, which can result in degradation, oxidation, and/or evaporation. The situation has been changed in 1997, by the discovery of interesting TE properties in the Na_xCoO₂ ceramic material [2]. Since then, great efforts have been performed to explore new TE materials, especially in the CoO-based families, with high TE performances. After these years, many works have been performed in layered cobaltites, such as [Ca₂CoO₃][CoO₂]_{1.62}, [Bi_{0.87}SrO₂]₂[CoO₂]_{1.82}, and [Bi₂Ba₂O₄][CoO₂]_{1.98} with promising TE properties [3-7].

The cobaltites crystal structure is formed by two different layers, which can be described as an alternate stacking of a common conductive CdI₂-type CoO₂ layer with a two-dimensional triangular lattice, and a block layer, composed of insulating rock-salt-type (RS) layers. These two sublattices possess common a- and c-axis lattice parameters and β angles while having different b-axis length, causing a misfit along the b-direction [7-9]. As a consequence, layered cobaltites possess a very high crystallographical anisotropy which, in turn, produces a high electrical one. For this reason, the alignment of their plate-like grains is essential to attain macroscopic properties comparable to those obtained on single crystals. Some methods have been shown to be adequate to obtain a good grain orientation in oxide ceramics, as template grain growth (TGG) [10], spark plasma sintering [11], directional growth from the melt [12], or the electrically

assisted laser floating zone method, EALFZ [13]. All texturing techniques, when applied in optimal conditions, produce well oriented grains which lead to the decrease on the electrical resistivity in the texturing direction. Concretely, the samples grown by the laser floating zone technique show a reduction of electrical resistivity due to the good orientation and large grain sizes [14]. On the other hand, previous studies on electrically assisted laser grown samples have shown that the current polarity strongly influences the samples microstructure and performances [15]. The aim of the present work is studying the evolution of microstructure and TE performances of $\text{Bi}_2\text{Ca}_2\text{Co}_{1.7}\text{O}_x$ textured ceramics when an electrical current intensity is applied during the growth process. $\text{Bi}_2\text{Ca}_2\text{Co}_{1.7}\text{O}_x$ polycrystalline samples were prepared using the classical solid-state route from commercial Bi_2O_3 (Panreac, 98+%), BaCO_3 (Panreac, 99+%), and Co_2O_3 (Aldrich, 98+%) powders. They were weighed in the appropriate proportions, mixed and ball milled in acetone media at 300rpm for 30 minutes to produce a homogeneous mixture. The obtained powders suspension was then dried in a fast IR evaporation system. The remaining powder was manually ground and thermally treated twice, under air, at 750 and 800°C for about 12 hours, with an intermediate manual milling. The objective of this process is assuring the calcium carbonate decomposition [16], otherwise it would decompose in the molten zone, producing CO_2 bubbles inside the melt in the LFZ process, leading to the solidification front destabilization. The thermally treated powders were then milled, introduced into a latex tube (inner diameter ~3mm), and isostatically cold pressed at 200MPa for one minute to obtain green ceramic cylinders (~100mm long). The resulting cylinders were subsequently used as feed in a EALFZ device equipped with a continuous power CO_2 laser ($\lambda=10.6\mu\text{m}$, Spectron SLC) with an external DC power supply (ISO TECH IPS 603) which is described elsewhere [17].

All the EALFZ grown samples were processed, with 0 and 300mA applied current, at 30mm/h under air, with a seed rotation of 3rpm anticlockwise while the feed was rotated at 15rpm, in the opposite direction, in order to assure the molten zone compositional homogeneity. After the texturing process, long (~100mm) and geometrically homogeneous (~2mm diameter) textured cylindrical rods have been produced. Finally,

the textured bars were cut into pieces with the adequate dimensions for their TE characterization (~15mm long pieces).

The grain orientation in textured samples has been determined on transversal sections of the samples by pole figures performed on the (020) diffraction peak, in a Philips X'Pert MRD X-ray diffractometer ($\text{CuK}\alpha$ radiation). Microstructures have been observed using a scanning electron microscope (SEM, Hitachi SU 70) equipped with an energy X-ray dispersive spectroscopy (EDS) system. Longitudinal polished sections of textured samples have been observed to evaluate the spatial phases distribution. Different contrasts have been studied by EDS to approximately determine their composition. Electrical resistivity and Seebeck coefficient have been simultaneously determined by the standard dc four-probe technique in a LSR3 measurement system (Linseis GmbH) under He atmosphere, in the steady state mode, at temperatures ranging from 50 (~room temperature) to 650°C. Samples performances have been determined through the power factor ($\text{PF} = S^2/\rho$), calculated from the previously measured electrical resistivity and Seebeck coefficient data.

Pole figures of the $\text{Bi}_2\text{Ca}_2\text{Co}_{1.7}\text{O}_x$ textured samples grown with 0 and 300mA are displayed in Figs. 1a and b, respectively. From the plot it is very clear that the applied current possess a beneficial effect on the grain alignment. The increased grain orientation with respect to the growth axis is reflected in a narrower central peak in the 300mA samples pole figure, compared with the ones grown without current.

The improvement in the grain orientation can be observed in Figs. 1c and d where SEM micrographs performed on polished longitudinal sections of the 0 and 300 mA samples are shown. At first sight it is easily observed that grains are better oriented with the rod axis when the electrical current is applied. On the other hand, when the micrographs are observed in detail, it is clear that it is possible to identify three different contrasts in the samples grown without current, as reported in previous works [13]. EDS analysis has shown that each of the contrasts corresponds to a different phase with compositions corresponding to the thermoelectric $\text{Bi}_2\text{Ca}_2\text{Co}_{1.7}\text{O}_x$ (grey contrast, #1), and to the non thermoelectric secondary ones $\text{Bi}_6\text{Ca}_4\text{O}_{13}$ and Co_3O_4 (light grey, #2, and dendritic-like black ones, #3, respectively). The relative amount of each one of these phases has been performed by image analysis of several micrographs and it has shown that

$\text{Bi}_2\text{Ca}_2\text{Co}_{1.7}\text{O}_x$ is in about 52.5 vol.%, $\text{Bi}_6\text{Ca}_4\text{O}_{13}$, 45.0 vol.%, and Co_3O_4 , 2.5 vol.%. On the other hand, the microstructural modifications induced by the 300mA during the growth process can be observed in Fig. 1d, where the phase #3 (Co_3O_4) disappears and very thin and long black grains are appearing (#4), associated to the thermoelectric $\text{Ca}_3\text{Co}_4\text{O}_9$ phase. The appearance of this last phase is indicative of the modifications, induced by the applied current, on the phase equilibrium as it has never been reported before, in our knowledge, the formation of $\text{Ca}_3\text{Co}_4\text{O}_9$ in the $\text{Bi}_2\text{Ca}_2\text{Co}_{1.7}\text{O}_x$ system. The relative amounts of the phases in the 300mA grown samples have been estimated as 40, 42, and 18 vol.% for $\text{Bi}_2\text{Ca}_2\text{Co}_{1.7}\text{O}_x$, $\text{Bi}_6\text{Ca}_4\text{O}_{13}$, and $\text{Ca}_3\text{Co}_4\text{O}_9$, respectively. These values indicate a slight decrease of secondary phases, compared with the proportion obtained on samples grown without current, and a raise of the amount of TE phases. The electrical resistivity of all the samples as a function of temperature is shown in Fig. 2. In the graph, it can be seen that the sample grown without current exhibit semiconductor-like behavior ($\delta\rho/\delta T < 0$) in all the measured temperature range, which is the typical one for this kind of materials [18]. When the external current is applied during the growth process, the electrical resistivity values decrease significantly (~80%) when compared with samples grown without current. Moreover, the samples behavior changes from the semiconducting-like one to a nearly temperature independent resistivity values. This evolution can be easily explained by the data obtained from the pole figures and the SEM micrographs, which show an increase on the grain alignment when the 300mA external electrical intensity is applied. The effect of this improvement of the grain alignment is reinforced by the slight decrease on the secondary phases content and the presence of the $\text{Ca}_3\text{Co}_4\text{O}_9$ phase which is known to possess lower electrical resistivity than the $\text{Bi}_2\text{Ca}_2\text{Co}_{1.7}\text{O}_x$ one. In any case, it is important to highlight that the lowest resistivity value obtained for the samples grown with 300 mA at room temperature, ~20m Ω .cm, is only slightly higher than the one obtained on $\text{Bi}_2\text{Ca}_2\text{Co}_2\text{O}_x$ single crystals at the same temperature, around 11m Ω .cm [19].

In Fig. 2 the Seebeck coefficient variation, as a function of temperature is also shown for all samples. At first sight it can be clearly seen that the values are positive in the whole measured temperature range, indicating a conduction mechanism predominantly governed by holes. Moreover, the thermopower values increase when temperature is

raised, with similar behavior for both types of samples. Other interesting feature, which can be observed in the figure, is that Seebeck coefficient decreases in about 25% at room temperature for the samples grown with external applied current, compared with the ones grown without current. This behavior is in agreement with the electrical resistivity evolution discussed previously. Anyway, all the samples show higher thermopower values at room temperature (~ 250 and $175 \mu\text{V/K}$ for samples grown without current and with 300mA, respectively) than the reported for $\text{Bi}_2\text{Ca}_2\text{Co}_2\text{O}_x$ single crystals ($150 \mu\text{V/K}$ at the same temperature) [19]. The large thermopower values measured in these samples are due to the large amount of oxygen vacancies in the thermoelectric $\text{Bi}_2\text{Ca}_2\text{Co}_{1.7}\text{O}_x$ phase produced by the laser floating zone technique [20]. The rise of the oxygen vacancies concentration promotes changes on Co oxidation state from Co^{4+} to Co^{3+} , thus increasing thermopower values, in agreement with Koshibae equation [21]. On the other hand, the presence of $\text{Ca}_3\text{Co}_4\text{O}_9$ phase, which usually exhibits higher thermopower than the $\text{Bi}_2\text{Ca}_2\text{Co}_{1.7}\text{O}_x$ one, in the samples grown with 300mA contributes to increase the Seebeck coefficient in these samples, compared with those grown without current.

Thermoelectric performances of both kinds of samples were evaluated through the power factor values. They were calculated from the electrical resistivity and thermopower data and presented, as a function of temperature, in Fig. 3. In this plot it can be clearly seen that all the samples show similar evolution and PF increases when the temperature is raised. When considering the PF values at room temperature, they increase from $\sim 0.06 \text{ mW/K}^2 \cdot \text{m}$ for samples textured without current to $\sim 0.17 \text{ mW/K}^2 \cdot \text{m}$ for samples grown with 300mA due to the large difference found in the electrical resistivity values. The maximum room temperature PF value is $\sim 20\%$ higher than the obtained on $\text{Bi}_2\text{Ca}_2\text{Co}_2\text{O}_x$ single crystals, $\sim 0.15 \text{ mW/K}^2 \cdot \text{m}$ [19]. This important improvement is due to the relatively small electrical resistivity values, together with the unusually high thermopower values discussed previously. The highest PF values ($\sim 0.3 \text{ mW/K}^2 \cdot \text{m}$) have been obtained at 650°C on the samples grown with 300mA which are more than two times higher than the obtained on the samples grown without electrical current. Moreover, this PF value is the highest one reported in $\text{Bi}_2\text{Ca}_2\text{Co}_{1.7}\text{O}_x$ polycrystalline

materials so far in our knowledge, making this kind of materials processed by EALFZ good candidates to be applied in practical devices.

In summary, this work demonstrates that a new thermoelectric composite can be successfully grown by EALFZ technique from a nominal $\text{Bi}_2\text{Ca}_2\text{Co}_{1.7}\text{O}_x$ composition. The applied external current strongly modifies the crystallization process, promoting the formation of $\text{Bi}_2\text{Ca}_2\text{Co}_{1.7}\text{O}_x + \text{Ca}_3\text{Co}_4\text{O}_9$ thermoelectric phases with improved grain alignment. Both factors lead to an important decrease on electrical resistivity, compared with the values measured on samples grown without current. In all cases Seebeck coefficient is higher than the obtained on single crystals due to the formation of oxygen vacancies. The best power factor values were obtained on samples grown at 300mA, $\sim 0.18 \text{ mW/K}^2 \cdot \text{m}$, at room temperature and $0.3 \text{ mW/K}^2 \cdot \text{m}^{-1}$ at 650°C which are the highest reported value for $\text{Bi}_2\text{Ca}_2\text{Co}_{1.7}\text{O}_x$ polycrystalline materials, in our knowledge.

The work was supported by the cooperation projects: E-41/11 and AIB2010-PT-00247. Sh. Rasekh acknowledges a JAEPre-2010 fellowship from the CSIC. A. Sotelo, M. A. Madre, J. C. Diez, and Sh. Rasekh acknowledge the Gobierno de Aragon (Grupos de Investigacion consolidados T12 and T87) funding. The authors gratefully acknowledge Marta Ferro for her assistant on SEM/EDS analysis, using the equipment supported by FCT Project REDE/1509/RME/2005. The authors acknowledge the financial support from the Portuguese Science and Technology Foundation (FCT) through the program PEst-C/CTM/LA0025/2011.

References

- [1] Rowe DM. In: Rowe DM, editor. Thermoelectrics handbook: macro to nano. 1st ed. Boca Raton, FL: CRC Press; 2006. p. 1-3.
- [2] I. Terasaki, Y. Sasago, and K. Uchinokura, Phys. Rev. B 56 (1997) 12685.
- [3] R. Funahashi, I. Matsubara, H. Ikuta, T. Takeuchi, U. Mizutani, S. Sodeoka, Jpn. J. Appl. Phys. 39 (2000) L1127.
- [4] J.C. Diez, Sh. Rasekh, M.A. Madre, E. Guilmeau, S. Marinel, A. Sotelo, J. Electron. Mater. 39 (2010) 1601.
- [5] A. Sotelo, E. Guilmeau, M.A. Madre, S. Marinel, J.C. Diez, M. Prevel, J. Eur. Ceram. Soc. 27 (2007) 3697.
- [6] A. Maignan, D. Pelloquin, S. Hébert, Y. Klein, M. Hervieu, Bol. Soc. Esp. Ceram. V. 45 (2006) 122.
- [7] W. Kobayashi, S. Hebert, H. Muguerra, D. Grebille, D. Pelloquin, A. Maignan, Thermoelectric properties in the misfit-layered-cobalt oxides $[\text{Bi}_2\text{A}_2\text{O}_4][\text{CoO}_2]_{b1/b2}$ (A=Ca, Sr, Ba, $b(1)/b(2)=1.65, 1.82, 1.98$) single crystals. In: I. Kim I (Ed.), Proceedings ICT 07: 26th international conference on thermoelectrics, IEEE, New York, 2008, pp. 117–20.
- [8] A. Maignan, S. Hebert, M. Hervieu, C. Michel, D. Pelloquin, D. Khomskii, J. Phys.: Condens. Matter; 15 (2003) 2711.
- [9] H. Itahara, C. Xia, J. Sugiyama, T. Tani, J. Mater. Chem. 14 (2004) 61.
- [10] Y. Masuda, D. Nagahama, H. Itahara, T. Tani, W. S. Seo, K. Koumoto, J. Mater. Chem. 13 (2003) 1094.
- [11] J. G. Noudem, D. Kenfau, D. Chateigner, M. Gomina, J. Electronic Mater. 40 (2011) 1100.
- [12] J.C. Diez, E. Guilmeau, M.A. Madre, S. Marinel, S. Lemonnier, A. Sotelo, Solid. State. Ionics. 180 (2009) 827.
- [13] N.M. Ferreira, Sh. Rasekh, F.M. Costa, M.A. Madre, A. Sotelo, J.C. Diez, M.A. Torres, Mater. Lett. 83 (2012) 144.
- [14] A. Sotelo, E. Guilmeau, Sh. Rasekh, M. A. Madre, S. Marinel, J. C. Diez, J. Eur. Ceram. Soc. 30 (2010) 1815.
- [15] N.M. Ferreira, Sh. Rasekh, A.J.S Fernandes, F.M. Costa, M.A. Madre, J.C. Diez, A.

Sotelo, *Microsc. Microanal.* 18 (2012) 93

[16] A. Sotelo, E. Guilmeau, M.A. Madre, S. Marinel, J.C. Diez, *Bol. Soc. Esp. Ceram.* V. 47 (2008) 225.

[17] M. F. Carrasco, R. A. Silva, R. F. Silva, V. S. Amaral and F. M. Costa, *Physica C* 460-462 (2007) 1347.

[18] A. Sotelo, Sh. Rasekh, E. Guilmeau, M.A. Madre, M.A. Torres, S. Marinel, J.C. Diez, *Mater. Res. Bull.* 46 (2011) 2537.

[19] E. Guilmeau, M. Pollet, D. Grebille, D. Chateigner, B. Vertruyen, R. Cloots, R. Funahashi, B. Ouladiaff, *Mater. Res. Bull.* 43 (2008) 394.

[20] Sh. Rasekh, M.A. Madre, J.C. Diez, E. Guilmeau, S. Marinel, A. Sotelo A, *Bol. Soc. Esp. Ceram.* V. 49 (2010) 371.

[21] W. Koshibae, K. Tsutsui, S. Maekawa, *Phys. Rev. B* 62 (2000) 6869.

Figure captions

Figure 1. Pole figure of cross sections of $\text{Bi}_2\text{Ca}_2\text{Co}_{1.7}\text{O}_x$ samples grown with: a) 0; and b) 300 mA

Figure 2. General SEM micrographs performed on longitudinal polished sections of $\text{Bi}_2\text{Ca}_2\text{Co}_{1.7}\text{O}_x$ samples grown with: a) 0; and b) 300 mA. Different phases identified by EDS are: #1 $\text{Bi}_2\text{Ca}_2\text{Co}_{1.7}\text{O}_x$; #2 $\text{Bi}_6\text{Ca}_4\text{O}_{13}$; #3 Co_3O_4 ; and #4 $\text{Ca}_3\text{Co}_4\text{O}_9$.

Figure 3. Temperature dependence of the electrical resistivity (filled symbols) and Seebeck coefficient (open symbols) for $\text{Bi}_2\text{Ca}_2\text{Co}_{1.7}\text{O}_x$ textured samples as a function of current intensity: 0 (● and ○) and 300mA (■ and □).

Figure 4. Temperature dependence of the power factor for $\text{Bi}_2\text{Ca}_2\text{Co}_{1.7}\text{O}_x$ textured samples as a function of current intensity: 0 (●) and 300mA (■)

Figure 1

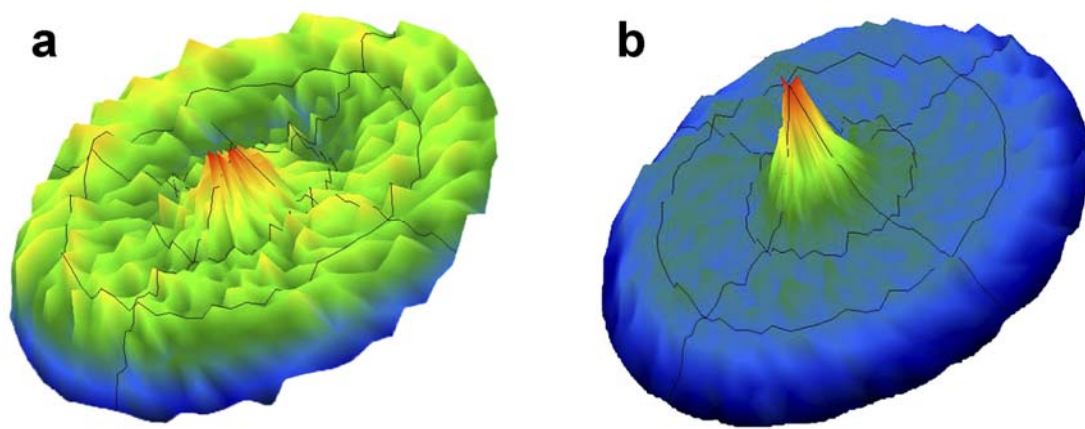


Figure 2

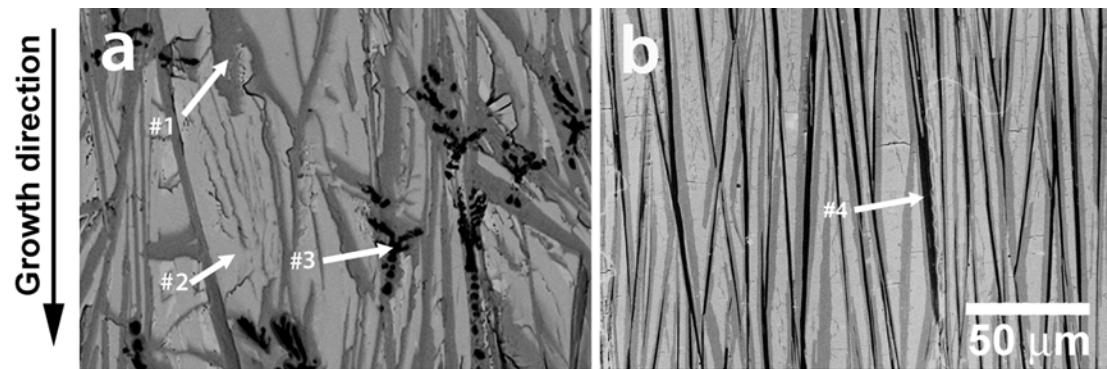


Figure 3

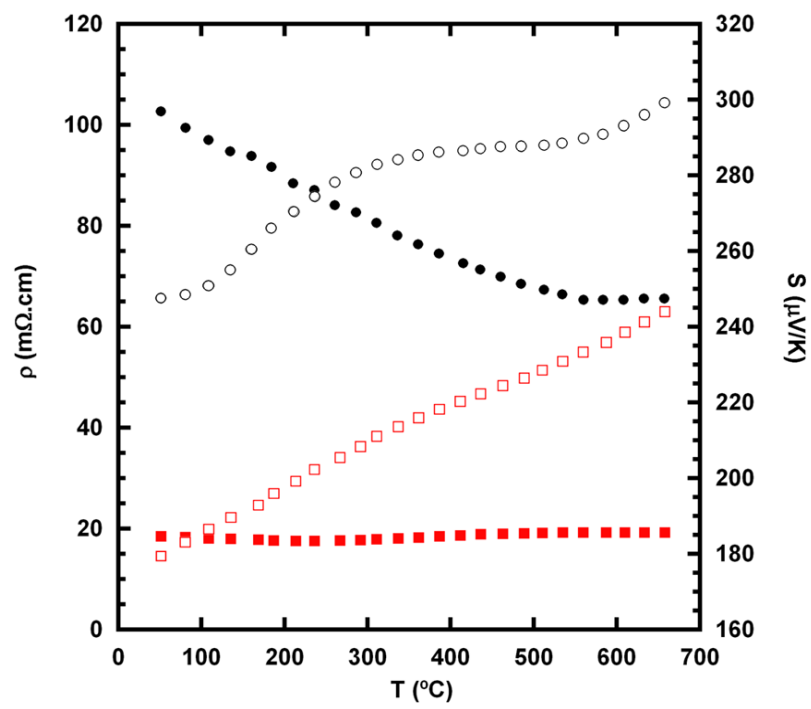


Figure 4

